

SVGFusion: Scalable Text-to-SVG Generation via Vector Space Diffusion

Ximing Xing, Juncheng Hu, Jing Zhang
Beihang University
{ximingxing, hujuncheng, zhang-jing}@buaa.edu.cn

Dong Xu
The University of Hong Kong
dongxu@cs.hku.hk

Qian Yu*
Beihang University
qianyu@buaa.edu.cn

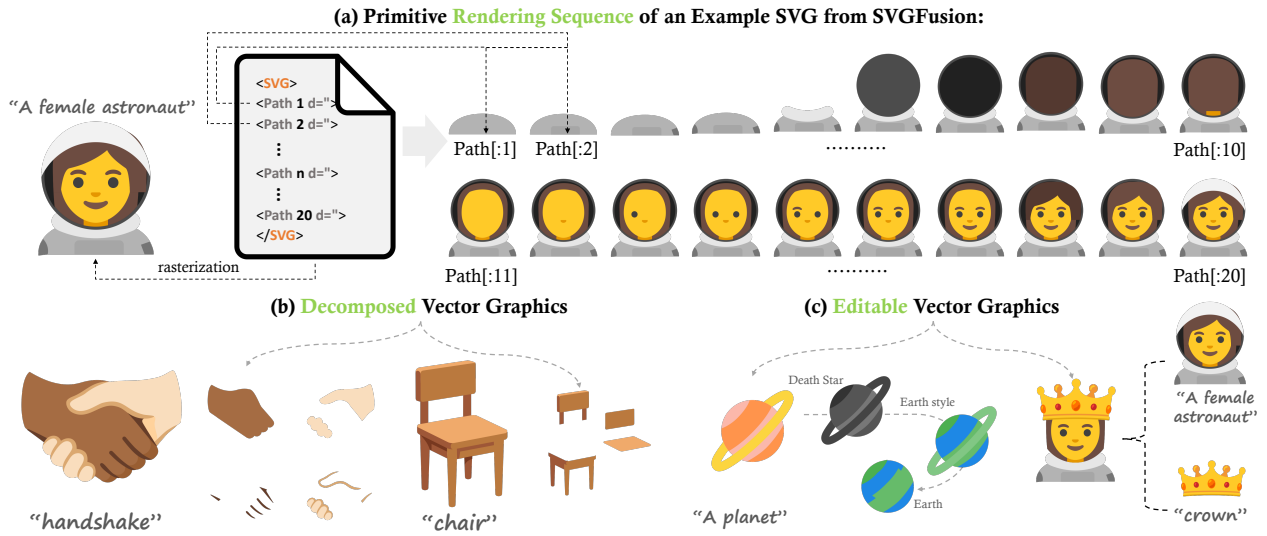


Figure 1. **Example SVGs generated by our SVGFusion.** Noteworthy characteristics of the SVGs generated by our new method include: (a) primitive ordering aligned with human design principles, (b) a clear and systematic layering structure of vector primitives, and (c) high editability.

Abstract

The generation of Scalable Vector Graphics (SVG) assets from textual data remains a significant challenge, largely due to the scarcity of high-quality vector datasets and the limitations in scalable vector representations required for modeling intricate graphic distributions. This work introduces SVGFusion, a Text-to-SVG model capable of scaling to real-world SVG data without reliance on a text-based discrete language model or prolonged SDS optimization. The essence of SVGFusion is to learn a continuous latent space for vector graphics with a popular Text-to-Image framework. Specifically, SVGFusion consists of two modules: a Vector-Pixel Fusion Variational Autoencoder (VP-VAE) and a Vector Space Diffusion Transformer (VS-DiT). VP-VAE takes both the SVGs and corresponding rasterizations as inputs and learns a continuous latent space, whereas

VS-DiT learns to generate a latent code within this space based on the text prompt. Based on VP-VAE, a novel rendering sequence modeling strategy is proposed to enable the latent space to embed the knowledge of construction logics in SVGs. This empowers the model to achieve human-like design capabilities in vector graphics, while systematically preventing occlusion in complex graphic compositions. Moreover, our SVGFusion’s ability can be continuously improved by leveraging the scalability of the VS-DiT by adding more VS-DiT blocks. A large-scale SVG dataset is collected to evaluate the effectiveness of our proposed method. Extensive experimentation has confirmed the superiority of our SVGFusion over existing SVG generation methods, achieving enhanced quality and generalizability, thereby establishing a novel framework for SVG content creation. Code, model, and data will be released at: <https://ximinng.github.io/SVGFusionProject/>

*Corresponding author.

1. Introduction

Scalable Vector Graphics (SVGs) have become essential in modern digital design, utilizing mathematical definitions to represent shapes such as paths, curves, and polygons instead of relying on pixel-based raster graphics. This vector-based approach enables SVGs to scale across resolutions without any loss of detail, offering precise quality control. Additionally, SVGs are efficient in terms of storage and transmission due to their compact structure, and they provide high levels of editability, allowing designers to make fine adjustments to graphic elements. As a result, SVGs play an essential role in applications like web design and user interfaces, including icons, logos, and emojis.

The task of SVG generation has attracted increasing attention in recent years. Existing methods can be categorized into two types: optimization-based and language model-based. Optimization-based methods [8, 18, 34, 46, 52, 56, 63, 64] generally initialize an SVG in vector space and then rasterize it into pixel space via differentiable rendering [19] for loss computation. Gradients are back-propagated to the vector space to update the parameters of the SVG. Although optimization-based methods can produce good results by leveraging priors from large pre-trained models like CLIP [34] or Stable Diffusion [38], they are very time-consuming. Moreover, limited by the use of differentiable rasterizers [19], these methods [18, 63–65] only consider a few types of ‘differentiable’ commands in SVGs, e.g., Cubic Bézier curves. Furthermore, the results generated by these methods are difficult to edit as the primitives often intertwine or occlude each other.

Alternatively, language model-based methods [3, 11, 50, 58, 59, 61] treat SVG generation as a sequential task and employ a language model, like RNNs or Transformers, to predict in an auto-regressive manner. However, these methods can become inefficient when the command sequence of an SVG is too long. Additionally, it is challenging for these models to learn the complex syntax and numerous primitive types without extensive data. Consequently, these methods often simplify the task by limiting SVG the representation to one primitive type, `<path>`, and three path commands: `Move to (M)`, `Line to (L)`, and `Cubic Bézier (C)`. This simplification mainly restricts their output to generating black-and-white icons and single-letter shapes, thus limiting their applicability in real-world SVG applications. Moreover, existing methods generally overlook the inherent creation logic of an SVG, leading to unreasonable constructions.

In this work, we propose **SVGFusion**, a novel model designed for text-based SVG generation. This model can output SVGs that are decomposable, editable, and

reflect human-like design logic, as demonstrated in Fig. 1. Inspired by the recent success of Latent Diffusion Models (LDMs) [38] in the Text-to-Image (T2I) task, our SVGFusion adopts an LDM-like framework wherein a continuous vector space is learned to generate SVGs. Specifically, SVGFusion comprises two core modules: a Vector-Pixel Fusion Variational Autoencoder (VP-VAE) and a Vector Space Diffusion Transformer (VS-DiT). The VP-VAE is tasked with learning a latent space for vector sketches, whereas the VS-DiT is responsible for generating a latent code within this space, conditioned on the input text prompt. This architecture enables our model to capitalize on the successes observed in the T2I tasks. The VP-VAE employs a transformer-based architecture, which enhances SVGFusion’s capability to effectively model the latent space and supports a broader range of primitives. Additionally, SVGFusion can continuously enhance its interpretive and generative capacities by leveraging the scalability of the VS-DiT, which can be expanded by adding more VS-DiT blocks.

More importantly, SVGFusion is capable of emulating human design principles in SVGs, ensuring more reasonable SVG construction and improved editability. To achieve this, we introduce a rendering sequence modeling strategy, where a batch learning unit is structured according to the SVG rendering sequence to simulate human design processes (as shown in Fig. 7). Furthermore, we incorporate visual data—that is, the rasterizations of the corresponding SVGs—and feed them along with the SVGs into our VP-VAE to learn a latent space that embeds human design principles. To simulate real-world SVG synthesis and evaluate our proposed method, we collected approximately 240,000 high-quality, human-designed SVGs, including color emojis and icons. We also established an automated processing pipeline for lossless data refinement. Extensive experiments demonstrate that SVGFusion not only enhances the visual quality of SVGs but also exhibits strong generalizability.

The contribution of this work is three-fold:

- **A Novel, Efficient, and Scalable SVG Generation Model:** We introduce SVGFusion, which adopts a popular Text-to-Image framework for Text-to-SVG generation. This model is not only efficient and scalable but also supports a broader range of SVG primitives.
- **Specific Module Design and Training Strategy to Learn Creation Logic:** To capture the creation logic of man-made SVGs and ensure reasonable SVG construction, we propose a novel Vector-Pixel Fusion Variational Autoencoder (VP-VAE) that processes both SVGs and their corresponding rasterizations. Additionally, a novel rendering sequence modeling strategy is implemented to prepare the training data.

To the best of our knowledge, this is the first Text-to-SVG model that explicitly considers the creation logic of SVGs.

- **A Large-Scale, High-Quality SVG Dataset and Comprehensive Evaluation:** We have curated a dataset of approximately 240k high-quality, human-designed SVGs and conducted extensive experiments to validate SVGFusion’s effectiveness in SVG generation, thereby setting a new benchmark for this task.

2. Related Work

2.1. Vector Graphics Generation

Scalable Vector Graphics (SVGs) are widely used in design due to their advantages, such as geometric manipulability, resolution independence, and compact file structure. One approach to SVG generation involves training neural networks to output predefined SVG commands and attributes [3, 11, 21, 36, 50, 61]. These networks typically use architectures like RNNs [11, 36], VAEs [21], and Transformers [3, 50, 61]. However, the lack of large-scale vector datasets limits their ability to generalize and create intricate graphics.

Currently, the vector graphics field lacks datasets comparable in scale to ImageNet [6], with most datasets focused on narrow areas such as monochromatic vector icons [5], emojis [9], and fonts [58]. An alternative to directly training an SVG generation network is optimizing to match a target image during the evaluation phase.

Li *et al.*[19] introduced a differentiable rasterizer to bridge vector graphics and raster images. Recent work has used differentiable rasterizers to overcome dataset limitations[16, 24, 46, 52, 63, 65]. This method optimizes SVG parameters based on a pretrained vision-language model. Advances in models like CLIP [34] have enabled successful sketch generation methods, such as CLIPDraw [8] and CLIPasso [56], while DreamFusion [33] has shown diffusion models’ superior generation abilities. VectorFusion [18], DiffSketcher [63], and SVGDreamer [64] combine differentiable rasterizers with text-to-image diffusion models to generate vector graphics, achieving promising results in iconography and sketching. However, these methods still suffer from limited editability and graphical quality. Recent studies [51, 65] have combined optimization-based approaches with neural networks to improve vector representations by incorporating geometric constraints. We propose SVGFusion, an innovative model for scalable SVG generation that operates in a continuous vector space, overcoming the limitations of discrete language models and intensive optimization techniques to generate high-quality SVGs at scale.

2.2. Diffusion Model

Denoising diffusion probabilistic models (DDPM) [7, 13, 14, 26, 38, 42–45] have demonstrated outstanding performance in generating high-quality images. The diffusion model architecture combined with the language-image pretrained model [34] shows obvious advantages in text-to-image (T2I) tasks, including GLIDE [27], Stable Diffusion [38], DALL-E 2 [35], Imagen [39] and DeepFloyd IF [47], SDXL [32]. The progress achieved by T2I diffusion models [27, 35, 38, 39] also promotes the development of a series of text-guided tasks, such as text-to-3D [33, 57, 60] and text-to-video [10, 15, 20, 41].

Recent efforts such as DreamFusion [33] explores text-to-3D generation by exploiting a Score Distillation Sampling (SDS) loss derived from a 2D text-to-image diffusion model [38, 39] instead, showing impressive results. In addition, Sora [20] based on the latent diffusion model [31] has made amazing progress in the field of video generation. Recently, the architecture of diffusion models has been shifting from U-Net [7] architectures to transformer-based architectures [2, 23, 31], narrowing the gap between image generation and language understanding tasks. In this work, we extend the diffusion transformer to the domain of vector graphics, enabling the synthesis of vector graphics. We also demonstrate the potential of the proposed method in vector design. However, the absence of a scalable foundation model for vector graphics has significantly hindered the development of this field for broader applications. To address this, we propose SVGFusion, a scalable foundation model based on vector space design.

3. Methods

General-purpose SVGs, often designed manually, are composed of numerous vector primitives, which creates substantial challenges for language models when modeling sequences directly in the SVG representation space due to increased computational demands. Drawing inspiration from recent advancements in T2I methods [31, 38] developed within latent spaces, this strategy facilitates the construction of longer sequences and the application of more intricate models.

As shown in Fig. 2, our SVGFusion pipeline proceeds through three main stages. (a) The pipeline begins by encoding SVGs into a neural representation. Here, XML-defined SVGs are converted into a learnable matrix to yield an SVG embedding. To introduce human design priors, we propose a rendering sequence modeling approach and construct pairs of SVG codes and their corresponding renderings. (b) We introduce the Vector-Pixel Fusion Variational Autoencoder (VP-VAE), a Transformer-based architecture that encodes both vector embeddings and pixel-level features into a

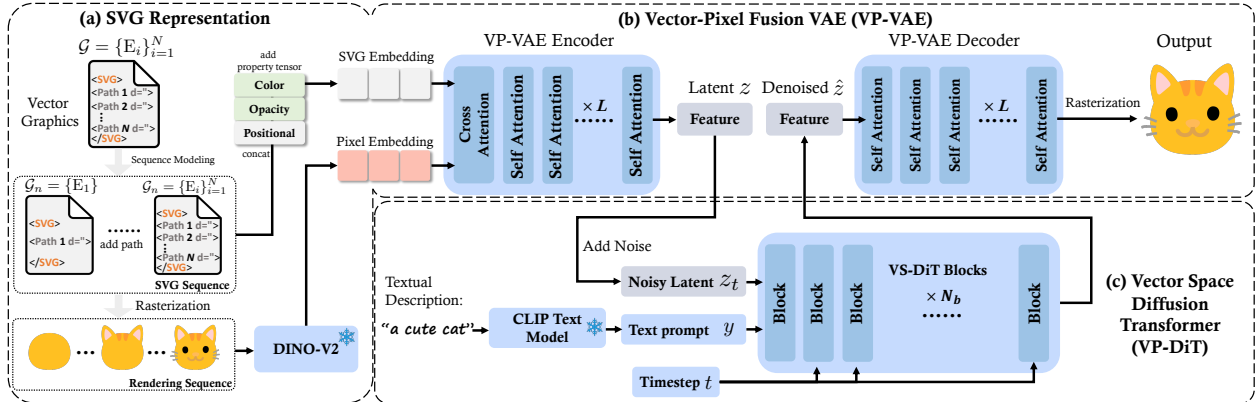


Figure 2. **An overview of our SVGFusion pipeline.** (a) Our pipeline begins with the neural representation of SVGs, where XML-defined SVG tensors are transformed into a learnable matrix to derive an SVG embedding (Sec.3.1). (b) We propose the Vector-Pixel Fusion Variational Autoencoder (VP-VAE, Sec.3.2) within a transformer-based architecture to encode vector embeddings alongside pixel-level features into a latent vector space. The resulting vectors are subsequently decoded using a transformer decoder, which parallels the encoder, to reconstruct vector graphics. (c) The Vector Space Diffusion Transformer (VS-DiT, Sec.3.3) is then trained within the latent space constructed by the VP-VAE. Textual features extracted from the text prompt using the CLIP[34] models are incorporated into each VS-DiT block. The generative capability of SVGFusion can be continuously enhanced by stacking additional VS-DiT blocks.

latent vector space. The encoded vectors are subsequently passed through a Transformer decoder, which parallels the encoder structure, to reconstruct vector graphics. (c) Finally, the Vector Space Diffusion Transformer (VS-DiT) is trained within the latent space established by the VP-VAE. Textual information is extracted from text prompts using the CLIP text encoder [34] and is incorporated into each VS-DiT block. Operating within this latent space, SVGFusion allows for flexible model scalability by enabling additional VS-DiT blocks to be stacked, thereby refining the generative performance.

Let an SVG file be defined as a collection of N vector primitives: $\text{SVG } \mathcal{G} = \{E_1, E_2, \dots, E_n\} = \{E_i\}_{i=1}^N$, where each E_i represents an *element-level* primitive, such as $\langle \text{path} \rangle$, $\langle \text{rect} \rangle$, $\langle \text{circle} \rangle$, etc. $E_i = \{S_{i,j}, F_{i,j}, \alpha_{i,j}\}_{j=1}^{M_i}$, where $S_{i,j}$ is the j -th *command-level* primitive in the i -th element, $F_i \in \{r, g, b\}$ is the i -th element color property and $\alpha_i \in \{0, 1\}$ is the visibility of the i -th element. M_i indicates the total number of commands in E_i . The element $\langle \text{path} \rangle$ may consist of several commands, while other elements consist of only one command.

3.1. SVG Representation

Vector graphics consist of machine instructions composed of a series of XML elements (*e.g.* $\langle \text{path} \rangle$ or $\langle \text{rect} \rangle$) and attributes (*e.g.* d , rx or ry), which we tensor quantize into a learnable matrix. Inspired by previous works [3, 58], we define an SVG in matrix form so that it can be easily represented by tensor quantization. While previous works [3, 58, 61] simplify the SVG mod-

eling task by limiting the command set, thereby constraining the generalizability of SVG representations, our work broadens the SVG element and command sets to accommodate a more extensive range of vector forms. This enhancement significantly improves the model’s ability to learn from real-world data.

SVG Embedding. In [3, 50, 58, 61], only a single SVG element, $\langle \text{path} \rangle$, is employed to approximate all other SVG elements, which inherently leads to information loss and reduces fidelity to human-created SVGs. To address this limitation, we extend the SVG element set beyond $\langle \text{path} \rangle$ to encompass multiple distinct elements (see Supplementary Sec. C), thereby enhancing the model’s adaptability and precision in representing complex SVG designs. We first transform the SVG code into an SVG matrix by converting each primitive to an individual vector with rules: $\vec{E}_i = \sum_{j=1}^{M_i} S_{i,j} = (\rho, \tau, \mu_0, \nu_0, \mu_1, \nu_1, \mu_2, \nu_2, \mu_3, \nu_3)_j^i$, where ρ and τ represent the element and command types, respectively. If ρ is the $\langle \text{path} \rangle$ element, then (μ_0, ν_0) and (μ_3, ν_3) represent the beginning and end points, while (μ_1, ν_1) and (μ_2, ν_2) are control points. Then, to establish interconnections among the adjacent commands, we set the end point of command (μ_3, ν_3) equal to the beginning point (μ_0, ν_0) of the subsequent command in each individual path. If ρ is $\langle \text{rect} \rangle$, then $(\mu_i, \nu_j)_{i=0, j=0}^{3,3}$ correspond to the width, height, x , y , rx , and ry , respectively. We decompose each SVG primitive into basic commands, combining them into a structured matrix form. This results in a structured SVG matrix $\mathcal{G} \in \mathbb{R}^{(\sum_i^N M_i) \times 10}$, where $\sum_i^N M_i$ indicates individual basic commands.

Rendering Sequence Modeling. Our goal is to develop an SVG synthesis method that aligns with human design logic and enables the model to learn SVG creation through imitative learning, by closely simulating the sequence in which humans draw vector graphic primitives. Specifically, we guide the model to construct SVGs incrementally, following the drawing order of primitives in real data, allowing it to observe progressive changes in the SVG structure across batch dimensions. In addition, we inject visual priors into the process. We use pre-trained DINOv2 [30] $f_{\text{dino}}(\cdot)$ to extract visual features from each SVG rendering and overlay them to form visual prior variations. Such design enables the model to learn the SVG drawing process through both visual and geometric changes. To enhance the model’s comprehension of sequential information, we incorporate rotary position embeddings (RoPE) [48], similar to those used in advanced large language models [28, 53], to capture dependencies across different sequence positions.

3.2. Vector-Pixel Fusion VAE

Sampling vector graphics in one-dimensional discrete vector spaces poses significant challenges for language models, as it requires handling complex dependencies across sparse and high-dimensional textual representations, making it difficult to capture the intricate structure and continuity inherent in vector graphics. Our goal is to learn the neural representation of vector graphics by mapping vector geometric features to the latent space. Unlike previous methods [3, 21, 58, 61], our approach overcomes two primary limitations: 1) the difficulty of capturing visual information in vector graphics through implicit latent representations, which often leads to sub-optimal quality in decoded SVG shapes; and 2) the challenges associated with training and sampling from an unstructured and under-constrained latent space. To achieve this, as shown in Fig. 2(b), we propose a Vector-Pixel Fusion Variational Autoencoder (VP-VAE) that learns the representations from both pixel features and vector primitives. Given the requirement to model serialized vector primitives, we employ Transformer-based architectures for both our encoders and decoders, leveraging recent findings that highlight the superiority of this approach [3, 31, 55].

Vector-Pixel Fusion Encoding. Our proposed VP-VAE encoder, $\mathcal{E}(\cdot)$, accepts two types of inputs: pixel embeddings extracted from SVG renderings and SVG embeddings derived from SVG codes. This design aligns visual features with geometric embedding features during the coding phase. The encoder architecture of the VP-VAE comprises one cross-attention layer followed by L self-attention layers. Specifically, the pixel embeddings initially query the SVG embeddings

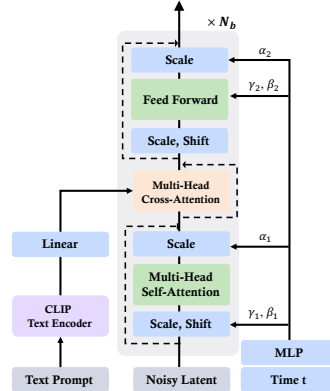


Figure 3. **The architecture of our VP-DiT Block.** A cross-attention module is integrated into each block to inject textual conditions.

through the cross-attention layer. The resulting tokens then pass through the subsequent self-attention layers. The final output latent code z from the encoder are designed to encapsulate both visual and geometric features.

SVG Decoding. The decoder of VP-VAE employs a similar structure to the encoder, but without the cross-attention layer. The latent code z is decoded into the SVG embeddings by the decoder. Finally, the reconstructed SVG embeddings are fed into a linear layer to predict the command and parameter logits.

VP-VAE Objective. We first quantify the differences between the predicted primitive E_i and the ground-truth primitive \hat{E}_i via cross-entropy loss. In addition to reconstruction losses associated with both components, the latent space undergoes regularization via a KL divergence loss. The final loss of VP-VAE is presented in Eq. 1:

$$\mathcal{L}_{\text{VAE}} = \mathcal{L}_{\text{CE}}(E_i, \hat{E}_i) + \lambda_{\text{KL}} \mathcal{L}_{\text{KL}} \quad (1)$$

where \mathcal{L}_{KL} encourages the latent code z to follow a Gaussian distribution $\mathcal{N}(\mathbf{0}, \mathbf{I})$, and λ_{KL} denotes the weight of KL regularization.

3.3. Vector Space Diffusion Transformer

SVGfusion adopts the DiT [31] as the base architecture and perform the diffusion process in the vector latent space. To allow textual features $f(\mathcal{P})$ to interact with vector features, similar to [4], we incorporate a multi-head cross-attention layer into the VS-DiT block. It is positioned between the self-attention layer and the feed-forward layer so that the model can flexibly interact with the text embedding extracted from the language model. Our architecture supports flexible stacking of N_b VS-DiT blocks, enabling models with varied parameter scales that allow SVGfusion to adaptively expand with increasing data volume, thus enhancing scalability with data growth. Given an input SVG through VP-VAE:

$\mathbf{z} = \mathcal{E}(\mathcal{G})$, diffused inputs $\mathbf{z}_t = \alpha_t \mathbf{z} + \sigma_t \epsilon, \epsilon \sim \mathcal{N}(\mathbf{0}, \mathbf{I})$ are constructed; α_t and σ_t define a noise schedule, parameterized via a diffusion-time t . Following LDM [38], our VP-DiT model predicts the noise ϵ of the noisy latent representation \mathbf{z}_t at time t , conditioned on text prompt y . The objective is shown in Eq. 2:

$$\mathcal{L}_{\text{ldm}} = \mathbb{E}_{\mathcal{E}(\mathbf{x}), y, t, \epsilon \sim \mathcal{N}(\mathbf{0}, \mathbf{I})} \left[\|\epsilon_\phi(\mathbf{z}_t, t, y) - \epsilon\|_2^2 \right] \quad (2)$$

where $t \sim \mathcal{U}(0, 1)$. When training the diffusion model, we randomly zero the y with a probability of 10% to use classifier-free guidance [13], which can improve the quality of conditional generation during inference.

4. Experiments

Overview. This section covers the key aspects of our model implementation, followed by a description of the dataset collection and preprocessing pipeline. We then evaluate the performance of SVGFusion in generating high-quality SVGs by comparing it to state-of-the-art methods, both quantitatively and qualitatively in Sec. 4.2 and Sec. 4.3. The evaluation also includes an architectural analysis and ablation studies to highlight the contributions of individual model components. **Implementation Details.** To ensure consistency across all SVG data, we adopted relative positional coordinates. The model parameters are initialized randomly and optimized using the AdamW optimizer (with $\beta_1 = 0.9$, $\beta_2 = 0.95$) at an initial learning rate of 3×10^{-4} . The learning rate is warmed up over the first 2000 steps and then decayed to 1.5×10^{-5} following a cosine schedule. Additionally, we applied weight decay of 0.1 for regularization and constrain gradients by clipping their norms to a maximum value of 2.0. Besides, we normalized the input SVG embeddings into the $[-1, 1]$ range to stabilize the training process. We utilized Transformers as the fundamental building block for VP-VAE. Both the encoders and decoders are based on the Transformer architecture, consisting of 4 layers, a feed-forward dimension of 512, and an embedding size of $d_E = 256$. To investigate scaling trends, we trained VP-DiT models at three different sizes: 0.16B, 0.37B, and 0.76B parameters. We trained VP-VAE for 100k steps using a total batch size of 64 across 2 A800 GPUs, requiring approximately one day. Subsequently, leveraging the trained VP-VAE, we trained VP-DiT for 500k steps with a batch size of 128 on 8 A800 GPUs, taking approximately three days. In the sampling phase, we used DDIM [43] to denoise 100 steps; dpm-solver [22] also supports 20-step de-noising for more efficient sampling.

4.1. SVG Data Collection and Representation

We collected a large-scale SVG dataset for model training and evaluation, which includes 240k high-quality

Method / Metric	FID↓	CLIPScore↑	Aesthetic↑	HPS↑	TimeCost↓
Evolution [52]	121.43	0.193	2.124	0.115	47min23s
CLIPDraw [8]	116.65	0.249	3.980	0.135	5min10s
DiffSketcher[63]	72.30	0.310	5.156	0.242	10min22s
LIVE+VF [18]	82.22	0.310	4.517	0.253	30min01s
VectorFusion [18]	84.53	0.309	4.985	0.264	10min12s
Word-As-Img [17]	101.22	0.302	3.276	0.151	5min25s
SVGDreamer [64]	70.10	0.360	5.543	0.269	35min12s
SVG-VAE [21]	76.22	0.190	2.773	0.101	1min
DeepSVG [3]	69.22	0.212	3.019	0.114	2min
Iconshop [61]	52.22	0.251	3.474	0.140	1min03s
StrokeNUWA [50]	89.10	0.300	2.543	0.169	19s
SVG-Fusion-S	9.62	0.373	5.250	0.275	24s
SVG-Fusion-B	5.77	0.389	5.373	0.281	28s
SVG-Fusion-L	4.64	0.399	5.673	0.290	36s

Table 1. **Quantitative Comparison of SVGFusion vs. State-of-the-Art Text-to-SVG Methods.** Our method uses dpm-solver [22] for 20-step denoising.



Figure 4. **Samples from our collected SVG dataset.** The collected data includes a variety of SVG element types.

SVGs with *emoji* and icon style. Further details of this new dataset are provided in Supplementary Sec. D. SVG data collected from the Internet is often noisy, and using it directly for learning can hinder the model’s representation capabilities. About half of the data in an SVG file is redundant for visual rendering, including: 1) temporary data from vector editing applications, 2) non-optimal structural representations, and 3) unused or invisible graphic elements. To address this, we propose a preprocessing pipeline that reduces SVG file size losslessly, targeting four key aspects: elements, attributes, paths, and outputs. A detailed example is shown in Fig. S6 of Supplementary. The collected dataset is highly diverse, as depicted in Fig. 4. In terms of visual complexity, it includes primitives that vary from simple to intricate. Regarding primitive representation, the dataset includes both Bézier curves expressed using `<path>` and basic shapes represented by `<circle>` and `<rect>`, etc. In terms of color representation, the dataset contains both black-and-white graphics and vibrant, harmonious color images. Additionally, in terms of semantics, it covers a wide range of subjects, including people, animals, objects, and symbols.

4.2. Quantitative Evaluation

We compare our proposed method with baseline methods using five quantitative indicators across three dimensions: (1) Visual quality of the generated SVGs, assessed by FID (Fréchet Inception Distance) [12]; (2)

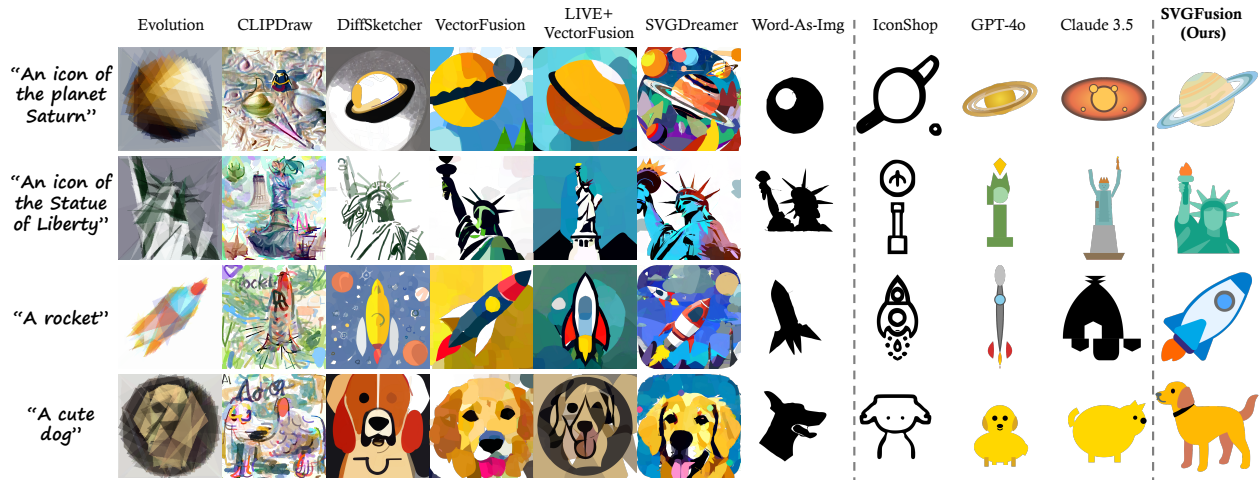


Figure 5. **Qualitative Comparison of SVGFusion and Existing Text-to-SVG Methods.** The target SVGs are in the *emoji* style. We use prompt modifiers for the optimization-based approach to encourage the appropriate style: “minimal flat 2D vector icon, emoji icon, lineal color, on a white background, trending on ArtStation.” Note that although the visual quality of results generated by optimization-based methods is high, these methods face challenges in decomposing the SVGs for further editing. **We encourage readers to zoom into this figure for a better illustration.**

Alignment with the input text prompt, assessed by CLIP score [34], and (3) Aesthetic appeal of the generated SVGs, measured by Aesthetic score [40] and HPS (Human Preference Score) [62]. To ensure a fair comparison, we also recorded the time cost of different methods to evaluate their computational efficiency.

Comparison results are presented in Table 1. The methods are categorized into two groups: optimization-based methods (top section of Table 1) and language model-based methods (middle section of Table 1). It is evident that our SVGFusion method surpasses other text-to-SVG methods across all evaluation metrics. This demonstrates the superiority of SVGFusion in generating vector graphics that are more closely aligned with text prompts and human preferences. Notably, compared to optimization-based methods, SVGFusion significantly reduces the time cost, enhancing its practicality and user-friendliness.

4.3. Qualitative Evaluation

Figure 5 presents a qualitative comparison between SVGFusion and existing text-to-SVG methods. The results are aligned with the quantitative results discussed in the previous section. Specifically, the methods Evolution [52], CLIPDraw [8], DiffSketcher [63], VectorFusion [18], LIVE [24]+VectorFusion [18], SVGDreamer [64], and Word-as-Img [17] are optimization-based, using a differentiable renderer [19] to backpropagate gradients to vector parameters. Evolution [52] and CLIPDraw [8] utilize CLIP [34] as the image prior, while DiffSketcher [63], VectorFusion [18], SVGDreamer [64], and Word-as-Img [17] adopt T2I diffu-



Figure 6. **Diffusion Process.** The diffusion process is visualized during model inference.

sion as the image prior. Despite their visual advantages, differentiable renderer-based methods often produce intertwined vector primitives, diminishing SVG editability. Iconshop [61], Claude 3.5 [29] and GPT4o [1] rely on language models, generate decoupled vector primitives but produce overly simplistic content.

It is worth noting that although optimization-based methods may produce more realistic or artistic visual effects, they rely on an LDM [38] sample as the target for optimization and require a differentiable rasterizer as the medium for this process. Additionally, they depend on differentiable vector primitives as the underlying representation for SVGs. As a result, these methods can only use `<path>` primitives described by Bézier curves. This leads to the need for a large amount of staggered overlapping primitives to closely fit the LDM sample, even for relatively simple shapes. Consequently, even simple regular shapes such as rectangular cannot be described using the corresponding basic shape primitives, thus losing the advantage of SVG’s editability, making it difficult to use in real-world scenarios.

In contrast, our approach not only ensures a clear SVG hierarchy but also maintains a balance between visual appeal and complexity. Figure 6 shows the process of denoising a vector graphic over timesteps. Starting

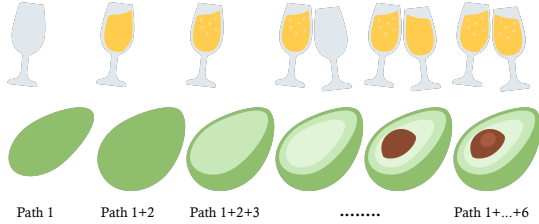


Figure 7. **Path Rendering Sequence.** SVGFusion is designed to align with human logic in SVG creation. The top diagram illustrates the left-to-right sequence of object placement, while the bottom diagram depicts the drawing order of an object from simple to complex.

with initial random, chaotic strokes, the elements of the SVG, such as vector coordinates, are progressively denoised at each timestep. After a period of denoising, the correct content is gradually restored while maintaining the visual harmony of the generated SVG.

As illustrated in Fig. 1(a) and Fig. 7, our SVGFusion can generate SVGs using only the necessary primitives, such as `<circle>` and `<rect>`. It allows for flexibility in the design process: one can either start by sketching the general shape and then add local details, or begin with a specific part and gradually add elements to complete the SVG. This approach coincides with the design process typically used by human designers when creating SVGs.

Comparison with Large Language Model. As illustrated in Fig. 5, we also compare our proposed SVGFusion with existing state-of-the-art approaches that directly generate SVGs using Large Language Models (LLMs). Claude 3.5 and GPT-4 are currently recognized as two of the best LLMs, but their performance in SVG generation is not particularly outstanding. In most cases, they can only use simple shapes to roughly assemble objects, but the positioning of each element lacks harmony. As a result, the overall shapes are overly simplistic, and the visual effects are less satisfactory. Regarding color design, these LLMs struggle to apply colors accurately to each part of the SVG, leading to color schemes that are often neither harmonious nor reasonable. In terms of semantic expression, the SVG code generated by LLMs is too simple to fully capture the meaning conveyed by the input text description. In contrast, our proposed SVGFusion method produces more balanced and harmonious results in terms of shape selection, color matching, and semantic representation. In Supplementary Sec. B, we provide more comparison of our method with language model-based methods.

Editability of SVGFusion Results. Figure 8 shows the editability of the SVG generated by our SVGFusion. Since the SVGs we generate have a clean and concise structure, we can easily edit the properties of the primitives, such as their color attributes. For instance, the

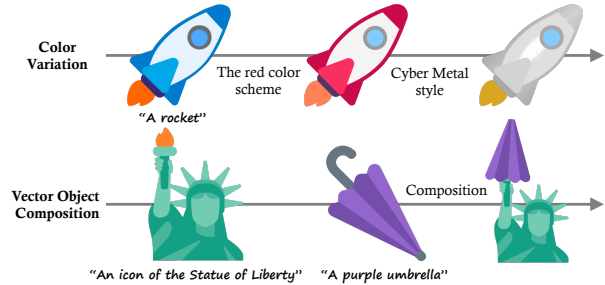


Figure 8. **The Editability of SVGFusion Results.** The SVGs generated by SVGFusion exhibit a clear hierarchical structure, thereby facilitating straightforward edits, such as color modifications (top example) or recombination into new graphics (bottom example).

Model	Layer N_b	Hidden size d	Heads	Gflops
VP-DiT S	12	384	6	1.4
VP-DiT B	12	768	12	5.6
VP-DiT L	24	1024	16	19.9

Table 2. **Details of VP-DiT Models.** We follow model configurations for the Small (S), Base (B) and Large (L) variants.

rocket we generated can be changed from blue to red, or even transformed into a cyber-metal style, simply by adjusting the color attributes. Furthermore, the capability of editability empowers users to efficiently reuse synthesized vector elements and create new vector compositions. As illustrated in the second example of Fig. 8, our method composes a new vector graphic by replacing the torch with a umbrella.

4.4. Ablation Study

Model Size. We apply a sequence of N DiT blocks, each operating at the hidden dimension size d . Following DiT [31], we use standard Transformer configs that jointly scale N , d and attention heads. Specifically, we use three configs: DiT-S, DiT-B, DiT-L. They cover a wide range of model sizes and flop allocations, from 1.4 to 19.9 Gflops, allowing us to gauge scaling performance. Table 2 gives details of the configs.

Comparison of Feature Extractors. As shown in Fig. 9, we utilize pretrained DINOv2 [30] as our feature extractor to capture precise geometric features of objects at the pixel level. In contrast, [58, 65] trained ConvNet for feature extraction, which was less effective at pixel-level characterization and introduced significant background noise.

We also conducted experiments to demonstrate the effectiveness of VP-VAE and Rendering Sequence Modeling. The results and analysis are provided in Supplementary Sec. A.

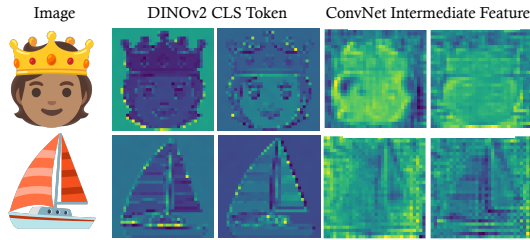


Figure 9. **Comparison of Feature Extractors.** We utilize pre-trained DINOv2 [30] as our feature extractor to capture precise geometric features of objects at the pixel level. In contrast, [58, 65] trained ConvNet for feature extraction, which was less effective at pixel-level characterization and introduced significant background noise.

5. Conclusion

In this work, we have presented SVGFusion, a novel generative model for scalable vector graphics (SVG) creation. By leveraging a continuous vector space and eliminating the need for text-based discrete language models or extensive optimization processes, SVGFusion significantly advances the state-of-the-art in SVG generation. Our model efficiently transforms textual SVG code into compact vector embeddings and captures the underlying distributional properties of encoded vectors through a diffusion process. Additionally, the integration of vector primitive rendering sequences allows for hierarchical interpretation, closely mimicking human-like design patterns and mitigating common issues such as occlusion in complex graphic compositions. Extensive experiments have demonstrated the superior performance and scalability of SVGFusion. We believe our SVGFusion offers a promising new framework for SVG content creation across a wide range of applications.

References

- [1] Josh Achiam, Steven Adler, Sandhini Agarwal, Lama Ahmad, Ilge Akkaya, Florencia Leoni Aleman, Diogo Almeida, Janko Altschmidt, Sam Altman, Shyamal Anadkat, et al. Gpt-4 technical report. *arXiv preprint arXiv:2303.08774*, 2023. 7
- [2] Fan Bao, Shen Nie, Kaiwen Xue, Yue Cao, Chongxuan Li, Hang Su, and Jun Zhu. All are worth words: A vit backbone for diffusion models. In *Proceedings of the IEEE/CVF Conference on Computer Vision and Pattern Recognition (CVPR)*, pages 22669–22679, 2023. 3
- [3] Alexandre Carlier, Martin Danelljan, Alexandre Alahi, and Radu Timofte. Deepsvg: A hierarchical generative network for vector graphics animation. *Advances in Neural Information Processing Systems (NeurIPS)*, 33: 16351–16361, 2020. 2, 3, 4, 5, 6, 12, 13
- [4] Junsong Chen, Jincheng YU, Chongjian GE, Lewei Yao, Enze Xie, Zhongdao Wang, James Kwok, Ping Luo, Huchuan Lu, and Zhenguo Li. Pixart- α : Fast training of diffusion transformer for photorealistic text-to-image synthesis. In *The Twelfth International Conference on Learning Representations (ICLR)*, 2024. 5
- [5] Louis Clouâtre and Marc Demers. Figr: Few-shot image generation with reptile. *arXiv preprint arXiv:1901.02199*, 2019. 3
- [6] Jia Deng, Wei Dong, Richard Socher, Li-Jia Li, Kai Li, and Li Fei-Fei. Imagenet: A large-scale hierarchical image database. In *2009 IEEE Conference on Computer Vision and Pattern Recognition (CVPR)*, pages 248–255, 2009. 3
- [7] Prafulla Dhariwal and Alexander Nichol. Diffusion models beat gans on image synthesis. *Advances in neural information processing systems (NeurIPS)*, 34:8780–8794, 2021. 3
- [8] Kevin Frans, Lisa Soros, and Olaf Witkowski. CLIP-Draw: Exploring text-to-drawing synthesis through language-image encoders. In *Advances in Neural Information Processing Systems (NeurIPS)*, 2022. 2, 3, 6, 7
- [9] Google. Noto emoji fonts. <https://github.com/googlefonts/noto-emoji>, 2014. 3, 13
- [10] Yuwei Guo, Ceyuan Yang, Anyi Rao, Zhengyang Liang, Yaohui Wang, Yu Qiao, Maneesh Agrawala, Dahua Lin, and Bo Dai. Animatediff: Animate your personalized text-to-image diffusion models without specific tuning. In *The Twelfth International Conference on Learning Representations (ICLR)*, 2024. 3
- [11] David Ha and Douglas Eck. A neural representation of sketch drawings. In *International Conference on Learning Representations (ICLR)*, 2018. 2, 3
- [12] Martin Heusel, Hubert Ramsauer, Thomas Unterthiner, Bernhard Nessler, and Sepp Hochreiter. Gans trained by a two time-scale update rule converge to a local nash equilibrium. *Advances in neural information processing systems (NeurIPS)*, 30, 2017. 6
- [13] Jonathan Ho and Tim Salimans. Classifier-free diffusion guidance. *arXiv preprint arXiv:2207.12598*, 2022. 3, 6
- [14] Jonathan Ho, Ajay Jain, and Pieter Abbeel. Denoising diffusion probabilistic models. In *Advances in Neural Information Processing Systems (NeurIPS)*, pages 6840–6851, 2020. 3
- [15] Jonathan Ho, Tim Salimans, Alexey Gritsenko, William Chan, Mohammad Norouzi, and David J Fleet. Video diffusion models. *Advances in Neural Information Processing Systems (NeurIPS)*, 35:8633–8646, 2022. 3
- [16] Teng Hu, Ran Yi, Baihong Qian, Jiangning Zhang, Paul L Rosin, and Yu-Kun Lai. Supersvg: Superpixel-based scalable vector graphics synthesis. In *Proceedings of the IEEE/CVF Conference on Computer Vision and Pattern Recognition (CVPR)*, pages 24892–24901, 2024. 3
- [17] Shir Iluz, Yael Vinker, Amir Hertz, Daniel Berio, Daniel Cohen-Or, and Ariel Shamir. Word-as-image for semantic typography. *ACM Transactions on Graphics (TOG)*, 42(4), 2023. 6, 7
- [18] Ajay Jain, Amber Xie, and Pieter Abbeel. Vectorfusion: Text-to-svg by abstracting pixel-based diffusion models. In *Proceedings of the IEEE/CVF Conference on Computer Vision and Pattern Recognition (CVPR)*, 2023. 2, 3, 6, 7

- [19] Tzu-Mao Li, Michal Lukáč, Gharbi Michaël, and Jonathan Ragan-Kelley. Differentiable vector graphics rasterization for editing and learning. *ACM Transactions on Graphics (TOG)*, 39(6):193:1–193:15, 2020. 2, 3, 7
- [20] Yixin Liu, Kai Zhang, Yuan Li, Zhiling Yan, Chujie Gao, Ruoxi Chen, Zhengqing Yuan, Yue Huang, Hanchi Sun, Jianfeng Gao, et al. Sora: A review on background, technology, limitations, and opportunities of large vision models. *arXiv preprint arXiv:2402.17177*, 2024. 3
- [21] Raphael Gontijo Lopes, David Ha, Douglas Eck, and Jonathon Shlens. A learned representation for scalable vector graphics. In *Proceedings of the IEEE/CVF International Conference on Computer Vision (ICCV)*, 2019. 3, 5, 6
- [22] Cheng Lu, Yuhao Zhou, Fan Bao, Jianfei Chen, Chongxuan Li, and Jun Zhu. Dpm-solver: A fast ode solver for diffusion probabilistic model sampling in around 10 steps. *Advances in Neural Information Processing Systems (NeurIPS)*, 35:5775–5787, 2022. 6
- [23] Nanye Ma, Mark Goldstein, Michael S Albergo, Nicholas M Boffi, Eric Vanden-Eijnden, and Saining Xie. Sit: Exploring flow and diffusion-based generative models with scalable interpolant transformers. In *Proceedings of the European Conference on Computer Vision (ECCV)*, 2024. 3
- [24] Xu Ma, Yuqian Zhou, Xingqian Xu, Bin Sun, Valerii Filev, Nikita Orlov, Yun Fu, and Humphrey Shi. Towards layer-wise image vectorization. In *Proceedings of the IEEE/CVF Conference on Computer Vision and Pattern Recognition (CVPR)*, pages 16314–16323, 2022. 3, 7
- [25] Microsoft. Fluent emoji. <https://github.com/microsoft/fluentui-emoji>, 2021. 13
- [26] Alexander Quinn Nichol and Prafulla Dhariwal. Improved denoising diffusion probabilistic models. In *International conference on machine learning (ICML)*, pages 8162–8171, 2021. 3
- [27] Alexander Quinn Nichol, Prafulla Dhariwal, Aditya Ramesh, Pranav Shyam, Pamela Mishkin, Bob McGrew, Ilya Sutskever, and Mark Chen. GLIDE: Towards photorealistic image generation and editing with text-guided diffusion models. In *Proceedings of the 39th International Conference on Machine Learning (ICML)*, pages 16784–16804, 2022. 3
- [28] OpenAI. Introducing chatgpt. <https://openai.com/index/chatgpt/>, 2023. 5
- [29] OpenAI. Claude 3.5 sonnet. <https://www.anthropic.com/news/claude-3-5-sonnet>, 2024. 7
- [30] Maxime Oquab, Timothée Darcet, Théo Moutakanni, Huy V. Vo, Marc Szafraniec, Vasil Khalidov, Pierre Fernandez, Daniel HAZIZA, Francisco Massa, Alaaeldin El-Nouby, Mido Assran, Nicolas Ballas, Wojciech Galuba, Russell Howes, Po-Yao Huang, Shang-Wen Li, Ishan Misra, Michael Rabbat, Vasu Sharma, Gabriel Synnaeve, Hu Xu, Herve Jegou, Julien Mairal, Patrick Labatut, Armand Joulin, and Piotr Bojanowski. DI-NOv2: Learning robust visual features without supervision. *Transactions on Machine Learning Research (TMLR)*, 2024. 5, 8, 9, 12
- [31] William Peebles and Saining Xie. Scalable diffusion models with transformers. In *Proceedings of the IEEE/CVF International Conference on Computer Vision (ICCV)*, pages 4195–4205, 2023. 3, 5, 8
- [32] Dustin Podell, Zion English, Kyle Lacey, Andreas Blattmann, Tim Dockhorn, Jonas Müller, Joe Penna, and Robin Rombach. SDXL: Improving latent diffusion models for high-resolution image synthesis. In *The Twelfth International Conference on Learning Representations (ICLR)*, 2024. 3
- [33] Ben Poole, Ajay Jain, Jonathan T. Barron, and Ben Mildenhall. Dreamfusion: Text-to-3d using 2d diffusion. In *The Eleventh International Conference on Learning Representations (ICLR)*, 2023. 3
- [34] Alec Radford, Jong Wook Kim, Chris Hallacy, Aditya Ramesh, Gabriel Goh, Sandhini Agarwal, Girish Sastry, Amanda Askell, Pamela Mishkin, Jack Clark, et al. Learning transferable visual models from natural language supervision. In *International Conference on Machine Learning (ICML)*, pages 8748–8763. PMLR, 2021. 2, 3, 4, 7
- [35] Aditya Ramesh, Prafulla Dhariwal, Alex Nichol, Casey Chu, and Mark Chen. Hierarchical text-conditional image generation with clip latents. *arXiv preprint arXiv:2204.06125*, 2022. 3
- [36] Pradyumna Reddy, Michael Gharbi, Michal Lukac, and Niloy J Mitra. Im2vec: Synthesizing vector graphics without vector supervision. In *Proceedings of the IEEE/CVF Conference on Computer Vision and Pattern Recognition (CVPR)*, pages 7342–7351, 2021. 3
- [37] ReShot. Reshot: Free icons & illustrations. <https://www.reshot.com/>, 2016. 13
- [38] Robin Rombach, Andreas Blattmann, Dominik Lorenz, Patrick Esser, and Björn Ommer. High-resolution image synthesis with latent diffusion models. In *Proceedings of the IEEE/CVF Conference on Computer Vision and Pattern Recognition (CVPR)*, pages 10684–10695, 2022. 2, 3, 6, 7
- [39] Chitwan Saharia, William Chan, Saurabh Saxena, Lala Li, Jay Whang, Emily L Denton, Kamyar Ghasemipour, Raphael Gontijo Lopes, Burcu Karagol Ayan, Tim Salimans, et al. Photorealistic text-to-image diffusion models with deep language understanding. In *Advances in Neural Information Processing Systems (NeurIPS)*, pages 36479–36494, 2022. 3
- [40] Christoph Schuhmann. Improved aesthetic predictor. <https://github.com/christophschuhmann/improved-aesthetic-predictor>, 2022. 7
- [41] Uriel Singer, Adam Polyak, Thomas Hayes, Xi Yin, Jie An, Songyang Zhang, Qiyuan Hu, Harry Yang, Oron Ashual, Oran Gafni, Devi Parikh, Sonal Gupta, and Yaniv Taigman. Make-a-video: Text-to-video generation without text-video data. In *The Eleventh International Conference on Learning Representations (ICLR)*, 2023. 3
- [42] Jascha Sohl-Dickstein, Eric Weiss, Niru Maheswaranathan, and Surya Ganguli. Deep unsupervised

- learning using nonequilibrium thermodynamics. In *Proceedings of the International Conference on Machine Learning (ICML)*, pages 2256–2265, 2015. 3
- [43] Jiaming Song, Chenlin Meng, and Stefano Ermon. Denoising diffusion implicit models. In *International Conference on Learning Representations (ICLR)*, 2021. 6
- [44] Yang Song and Stefano Ermon. Generative modeling by estimating gradients of the data distribution. In *Advances in Neural Information Processing Systems (NeurIPS)*, 2019.
- [45] Yang Song, Jascha Sohl-Dickstein, Diederik P Kingma, Abhishek Kumar, Stefano Ermon, and Ben Poole. Score-based generative modeling through stochastic differential equations. In *International Conference on Learning Representations (ICLR)*, 2021. 3
- [46] Yiren Song, Xuning Shao, Kang Chen, Weidong Zhang, Zhongliang Jing, and Minzhe Li. Clipvg: Text-guided image manipulation using differentiable vector graphics. In *Proceedings of the Conference on Artificial Intelligence (AAAI)*, 2023. 2, 3
- [47] StabilityAI. If by deepfloyd lab at stabilityai. <https://github.com/deep-floyd/IF>, 2023. 3
- [48] Jianlin Su, Murtadha Ahmed, Yu Lu, Shengfeng Pan, Wen Bo, and Yunfeng Liu. Roformer: Enhanced transformer with rotary position embedding. *Neurocomput.*, 568(C), 2024. 5
- [49] SVGRepo. Open-licensed svg vector and icons. <https://www.svgrepo.com/>, 2016. 13
- [50] Zecheng Tang, Chenfei Wu, Zekai Zhang, Mingheng Ni, Shengming Yin, Yu Liu, Zhengyuan Yang, Lijuan Wang, Zicheng Liu, Juntao Li, et al. Strokenuwa: Tokenizing strokes for vector graphic synthesis. *arXiv preprint arXiv:2401.17093*, 2024. 2, 3, 4, 6, 13
- [51] Vikas Thamizharasan, Difan Liu, Matthew Fisher, Nanxuan Zhao, Evangelos Kalogerakis, and Michal Lukac. Nivel: Neural implicit vector layers for text-to-vector generation. In *Proceedings of the IEEE/CVF Conference on Computer Vision and Pattern Recognition (CVPR)*, pages 4589–4597, 2024. 3
- [52] Yingtao Tian and David Ha. Modern evolution strategies for creativity: Fitting concrete images and abstract concepts. In *Artificial Intelligence in Music, Sound, Art and Design*, pages 275–291. Springer, 2022. 2, 3, 6, 7
- [53] Hugo Touvron, Thibaut Lavril, Gautier Izacard, Xavier Martinet, Marie-Anne Lachaux, Timothée Lacroix, Baptiste Rozière, Naman Goyal, Eric Hambro, Faisal Azhar, Aurelien Rodriguez, Armand Joulin, Edouard Grave, and Guillaume Lample. Llama: Open and efficient foundation language models. *ArXiv*, abs/2302.13971, 2023. 5
- [54] Twitter. Twitter color emoji svginot font. <https://github.com/13rac1/twemoji-color-font>, 2016. 13
- [55] Ashish Vaswani, Noam Shazeer, Niki Parmar, Jakob Uszkoreit, Llion Jones, Aidan N Gomez, Łukasz Kaiser, and Illia Polosukhin. Attention is all you need. In *Advances in Neural Information Processing Systems (NeurIPS)*. Curran Associates, Inc., 2017. 5
- [56] Yael Vinker, Ehsan Pajouheshgar, Jessica Y Bo, Roman Christian Bachmann, Amit Haim Bermano, Daniel Cohen-Or, Amir Zamir, and Ariel Shamir. Clipasso: Semantically-aware object sketching. *ACM Transactions on Graphics (TOG)*, 41(4):1–11, 2022. 2, 3
- [57] Haochen Wang, Xiaodan Du, Jiahao Li, Raymond A. Yeh, and Greg Shakhnarovich. Score jacobian chaining: Lifting pretrained 2d diffusion models for 3d generation. In *Proceedings of the IEEE/CVF Conference on Computer Vision and Pattern Recognition (CVPR)*, pages 12619–12629, 2023. 3
- [58] Yizhi Wang and Zhouhui Lian. Deepvecfont: Synthesizing high-quality vector fonts via dual-modality learning. *ACM Transactions on Graphics (TOG)*, 40(6), 2021. 2, 3, 4, 5, 8, 9, 13
- [59] Yuqing Wang, Yizhi Wang, Longhui Yu, Yuesheng Zhu, and Zhouhui Lian. Deepvecfont-v2: Exploiting transformers to synthesize vector fonts with higher quality. In *Proceedings of the IEEE/CVF Conference on Computer Vision and Pattern Recognition (CVPR)*, pages 18320–18328, 2023. 2, 13
- [60] Zhengyi Wang, Cheng Lu, Yikai Wang, Fan Bao, Chongxuan Li, Hang Su, and Jun Zhu. Prolificdreamer: High-fidelity and diverse text-to-3d generation with variational score distillation. In *Thirty-seventh Conference on Neural Information Processing Systems (NeurIPS)*, 2023. 3
- [61] Ronghuan Wu, Wanchao Su, Kede Ma, and Jing Liao. Iconshop: Text-based vector icon synthesis with autoregressive transformers. *arXiv preprint arXiv:2304.14400*, 2023. 2, 3, 4, 5, 6, 7, 12, 13
- [62] Xiaoshi Wu, Keqiang Sun, Feng Zhu, Rui Zhao, and Hongsheng Li. Human preference score: Better aligning text-to-image models with human preference. In *Proceedings of the IEEE/CVF International Conference on Computer Vision (ICCV)*, pages 2096–2105, 2023. 7
- [63] Ximing Xing, Chuang Wang, Haitao Zhou, Jing Zhang, Qian Yu, and Dong Xu. Diffsketcher: Text guided vector sketch synthesis through latent diffusion models. In *Advances in Neural Information Processing Systems (NeurIPS)*, 2023. 2, 3, 6, 7
- [64] Ximing Xing, Haitao Zhou, Chuang Wang, Jing Zhang, Dong Xu, and Qian Yu. Svgdreamer: Text guided svg generation with diffusion model. In *Proceedings of the IEEE/CVF Conference on Computer Vision and Pattern Recognition (CVPR)*, pages 4546–4555, 2024. 2, 3, 6, 7
- [65] Peiying Zhang, Nanxuan Zhao, and Jing Liao. Text-to-vector generation with neural path representation. *ACM Trans. Graph.*, 43(4), 2024. 2, 3, 8, 9

SVGFusion: Scalable Text-to-SVG Generation via Vector Space Diffusion

Supplementary Material

Overview

This supplementary material is organized into several sections, each providing additional details and analyses related to our work on **SVGFusion**. Specifically, it covers the following aspects:

- In Section A, we present the results of ablation studies to demonstrate the effects of VP-VAE and Rendering Sequence Modeling on the performance of SVGFusion.
- In Section B, we discuss the differences between the language model-based methods and our diffusion-based method, emphasizing how SVGFusion adopts an image-based paradigm to enhance SVG generation.
- In Section C, we demonstrate that SVGFusion supports a broader range of SVG primitives than existing methods, which enables it to capture the structural and visual characteristics of real-world SVGs more effectively.
- In Section D, we provide additional details about the new dataset and data cleaning process.
- In Section E, we present additional qualitative results of SVGFusion, demonstrating its capability to generate SVGs with high editability and visual quality.

A. Additional Ablation Studies

Ablation on VP-VAE. In SVGFusion, we introduce the Visual-Pixel Fusion Autoencoder (VP-VAE) to learn a continuous latent space for SVGs. This module processes both SVG primitive parameters and corresponding rasterized images as inputs, aligning the SVG codes with visual features during the encoding phase. In Fig. S1, we compare results with and without the integration of visual features. We observe that incorporating visual features leads to higher generation quality.

Ablation on Rendering Sequence Modeling. The Rendering Sequence Modeling strategy in SVGFusion is designed to simulate the order in which humans create vector graphic. By processing batches of SVGs with incrementally added primitives—alongside both SVG codes and corresponding rasterizations—our model can learn the logic behind SVG creation. In Fig. S1, we compare the effects of employing this strategy versus omitting it. The results clearly show more logical outcomes, e.g., the relationships between the scoops of ice cream, when Rendering Sequence Modeling is applied. This improvement is due to the order of primitives in our generated SVGs being more aligned with human creation logic.

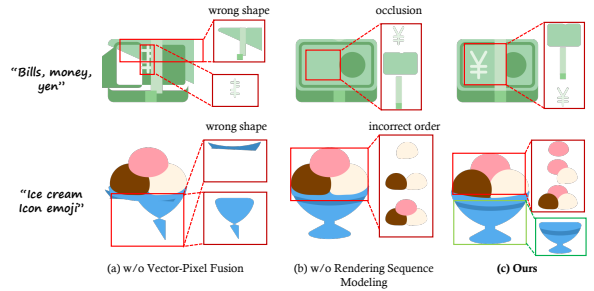


Figure S1. **Effects of VP-VAE and Rendering Sequence Modeling.** (a) vs. (c) demonstrates that without the Vector-Pixel Fusion (incorporating DINOv2 visual prior [30]), VP-VAE cannot accurately reconstruct or generate shapes. (a) vs. (c) indicates that employing Rendering Sequence Modeling results in more reasonable SVG outcomes, due to the order of primitives being better aligned with human creation logic.

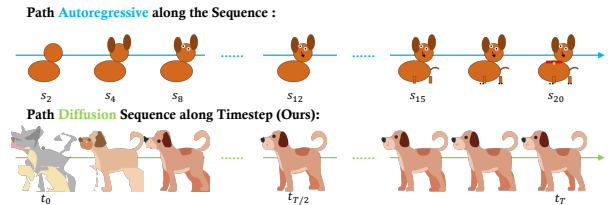


Figure S2. **Comparison of autoregressive language model prediction and diffusion-based generation of SVGFusion.**

B. Comparison with Language Model-based Methods

Language model-based methods such as DeepSVG [3] and IconShop [61] treat SVGs as sequences of tokens and predict outcomes in an autoregressive manner. However, the sequential nature of autoregressive approaches inherently limits them. As illustrated in the first row of Fig. S2, the prediction of each token heavily depends on the accuracy of the preceding tokens. Consequently, errors can propagate throughout the sequence, especially when initial predictions are suboptimal, ultimately leading to degraded performance.

Instead, our SVGFusion utilizes a diffusion-based approach to synthesize shapes in parallel rather than sequentially. As demonstrated in the first row of Fig. S2, this method circumvents the inherent limitations of autoregressive methods, effectively reducing the accumulation of errors.

C. More Primitive Types

SVG code comprises a suite of primitives and syntax rules. For example, the element-level primitive `<rect>` defines a rectangle shape with specified position, width, and height, and can be represented as `<rect x="10" y="20" width="50" height="80"/>`. However, given the multitude of SVG primitive types, it is challenging for Language Model-based methods to model these effectively due to the need for a complex data structure and extensive data. Consequently, some studies [3, 50, 58, 59, 61] simplify this task by focusing solely on one element-level primitive, `<path>`, and three command-level primitives: "Move To" (M), "Line To" (L), and "Cubic Bézier" (C). Such simplification is lossy and thereby those methods fail to accurately represent real SVGs as designed by humans.

To address these limitations, we have expanded the SVG representation in this work to support a broader range of SVG elements and commands. Specifically, as detailed in Table S1, our model now handles additional element-level commands such as `<circle>`, `<rect>`, and `<ellipse>`. Furthermore, as demonstrated in Figure S3, elements like `<line>`, `<polygon>`, and `<polyline>` can be losslessly converted into `<path>`. These elements are converted to `<path>` during the data preprocessing phase for consistency and efficiency.

Moreover, we have extended the path command set to include M (Move To), L (Line To), Q (Quadratic Bézier Curve), C (Cubic Bézier Curve), A (Arc To), and Z (Close Path). Other `<path>` commands, such as H (Horizontal Line To) and V (Vertical Line To), are losslessly represented by L, while S (Smooth Cubic Bézier Curve) and T (Smooth Quadratic Bézier Curve) are simplified versions of C and Q, respectively. These modifications streamline the process without sacrificing the accuracy of the representations.

D. SVG Dataset and Data Cleaning Process

SVG Dataset. The dataset consists of emoji and icon SVGs sourced from various sources, including Twemoji-Color-Font [54], Noto-Emoji [9], FluentUI-Emoji [25], SVG-Repo [49] and Reshot [37]. Twemoji-Color-Font, Noto-Emoji, and FluentUI-Emoji each contributes approximately 4,000 SVGs. An additional 30,000 SVGs are sourced from Reshot, while the majority—200,000 SVGs—are contributed by SVGRepo. These SVG resources are characterized by their high quality, rich color palettes, diverse designs, and human-designed nature, making them highly suitable for training and evaluation purposes.

Such a dataset enables us to design a model capable of leveraging prior knowledge of human-created SVGs

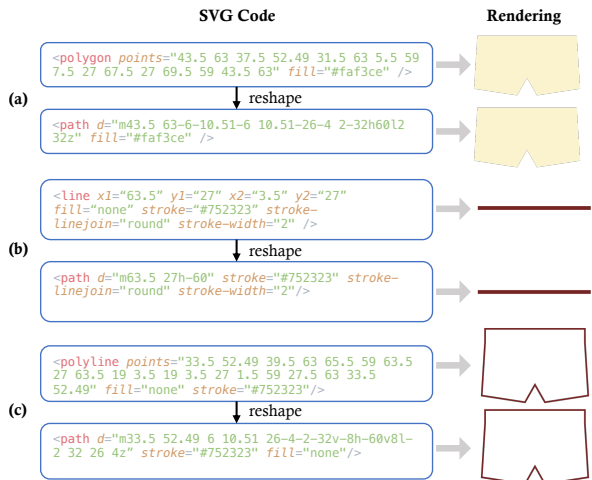


Figure S3. **Illustration of SVG primitive reshaping.** We show that (a) `<polygon>`, (b) `<line>`, and (c) `<polyline>` can be losslessly transformed into `<path>`.

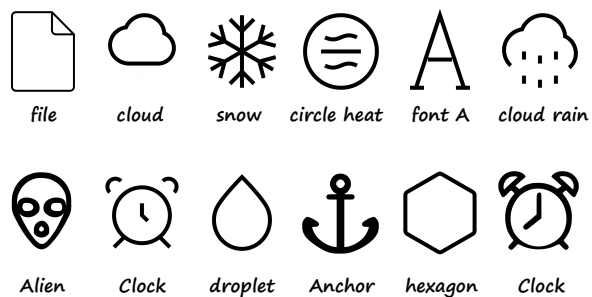


Figure S4. **SVG Icons Generated by SVG Fusion.**

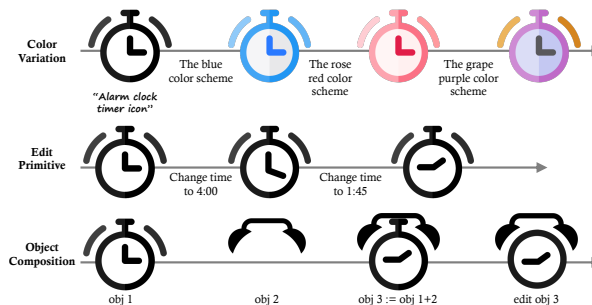


Figure S5. **The Editability of SVG Fusion Results.** The SVGs generated by SVG Fusion have a clear hierarchical structure, making them easy to edit, such as changing the colors (the top example) or recomposing into a new graphic (the bottom example).

to synthesize high-quality SVG outputs. However, SVG files collected from the web often contain noise, such as redundant data stemming from different designers' workflows. To address this, we apply a preprocessing step to remove redundancy, enhance training efficiency,

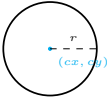


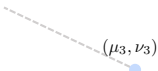
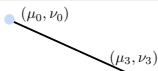
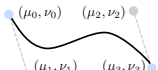
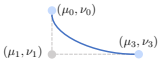
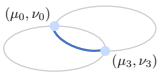
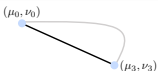
Primitive(element/command)	Argument	Explanation	Example
<code><circle></code>	r, cx, cy	The <code><circle></code> element is used to create a circle with center at (cx, cy) and radius r .	
<code><ellipse></code>	rx, ry, cx, cy	The <code><ellipse></code> element is used to create an ellipse with center at (cx, cy) , and radii rx and ry .	
<code><rect></code>	rx, ry, cx, cy	The <code><rect></code> element is used to create a rectangle, optionally with rounded corners if rx and ry are specified. The center is at (cx, cy) .	
<code><path> Move To (M)</code>	μ_3, ν_3	Moves the cursor to the specified point (μ_3, ν_3) .	
<code><path> Line To (L)</code>	μ_3, ν_3	Draws a line segment from the current point to (μ_3, ν_3) .	
<code><path> Cubic Bézier (C)</code>	$\mu_1, \nu_1, \mu_2, \nu_2, \mu_3, \nu_3$	Draws a cubic Bézier curve with control points (μ_1, ν_1) , (μ_2, ν_2) , and endpoint (μ_3, ν_3) .	
<code><path> Quadratic Bézier (Q)</code>	$\mu_1, \nu_1, \mu_2, \nu_2, \mu_3, \nu_3$	Draws a quadratic Bézier curve with control points (μ_1, ν_1) and endpoint (μ_3, ν_3) .	
<code><path> Elliptical Arc (A)</code>	$rx, ry, rotate, LargeArcFlag, SweepFlag, \mu_3, \nu_3$	Draws an elliptical arc from the current point to (μ_3, ν_3) . The ellipse has radii rx, ry , rotated by $rotate$ degrees. <code>LargeArcFlag</code> and <code>SweepFlag</code> control the arc direction.	
<code><path> Close Path (Z)</code>	\emptyset	Closes the path by moving the cursor back to the path's starting position (μ_0, ν_0) .	
<code><SOS></code>	\emptyset	Special token indicating the start of an SVG sequence.	N/A
<code><EOS></code>	\emptyset	Special token indicating the end of an SVG sequence.	N/A

Table S1. **SVG Primitives Supported by Our SVGFusion.** Compared to existing works, SVGFusion supports a broader range of elements (shown in the first three rows) and commands (shown in the 7th and 8th rows), which are highlighted in bold.

and ensure data consistency.

SVG Data Cleaning Process. The primary objective of the cleaning process is to perform lossless trimming of SVG files sourced from the web. Typically, more than half of the data in an SVG file is redundant and does not contribute to the rendering process. As illustrated in Figure S6, examples of rendering-irrelevant data include:

- 1) Temporary data generated by vector editing applications.
- 2) Suboptimal structural representations of SVG.
- 3) Unused or invisible graphical elements. These components are superfluous in finalized, published SVG files and can be safely removed to improve file efficiency.

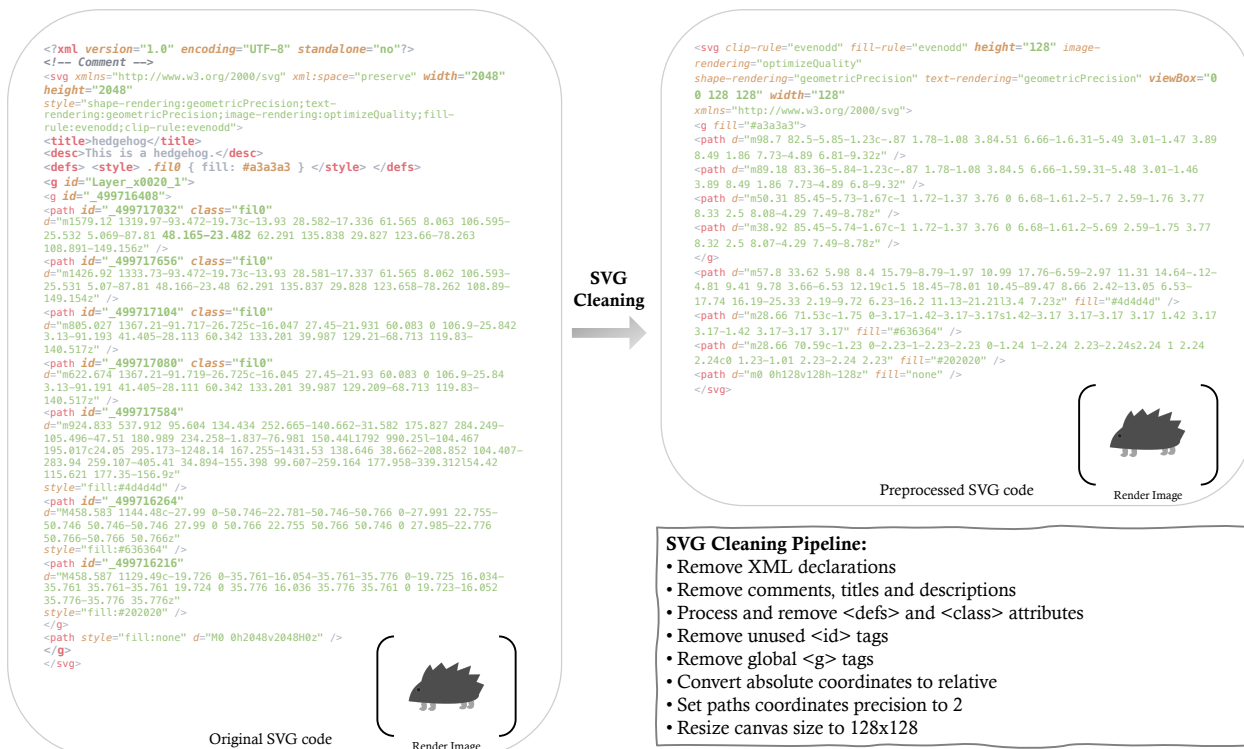


Figure S6. Description of the SVG cleaning process.

E. Additional Qualitative Results

Icon. As shown in Fig. S4, the proposed method is also adept at synthesizing simple icon-style SVGs, which are typically composed of a limited number of primitives and are defined by their minimalistic yet expressive design characteristics.

Editability. Fig. S5 demonstrates the high editability of SVGs produced by SVGFusion. The clean and systematic structure of these SVGs facilitates efficient modification of primitive properties, including color attributes, enabling seamless customization.

Conceptual Combination. The inherent editability of SVGFusion outputs enables users to efficiently repurpose synthesized vector elements and construct novel vector compositions. Notably, SVGs generated by SVGFusion can be seamlessly recombined to form entirely new designs, showcasing the flexibility and reusability of the framework.